www.icgst.com

Digital Optimal Compensation of Process Control Systems

Kamen M. Yanev[1]
Department of Electrical Engineering, University of Botswana, Gaborone, Botswana
yanevkm@yahoo.com, yanevkm@mopipi.ub.bw
http://www.ub.bw

Abstract

This paper is suggesting a practical method for realizing optimal digital compensation of process control systems. Initially, a cascade continuous compensator prototype is designed and further it is converted into its digital equivalent. The purpose of the compensator is to eliminate some properly selected poles of the original control system transfer function, to introduce new dominant poles and specific system amplification. As a result, the system's transient response and stability are considerably improved. The control system's relative damping ratio, percent maximum overshoot, phase margin, rise and settling times, are optimized.

Keywords: *Marginal system; Dominant poles; Stability; Analogue prototype; Lag-Lead multistage compensation; Digital compensation; Optimal system; Transient responses;*

Nomenclature

ITAE	Integral of the Time-weighted Absolute Error
ζ *(DR)*	Closed-loop relative damping ratio
PMO	Percent Maximum Overshoot
t_s	Settling time
t_m	Maximum overshoot time
e_{ss}	Steady-State error
$G_{P1}(s)$	Transfer function of the plant open-loop system
s	Laplace operator
K, K'	Variable gains of the linear system
$G_P(s)$	Characteristic equation of the open-loop system
$G_c(s)$	Transfer function of the analogue compensator
$G_c'(s)$	Transfer function of the multi-stage lead section of the compensator continuous prototype
$G_c''(s)$	Transfer function of the attenuation
$G_c'''(s)$	Transfer function of the of the lag compensation and amplification
T_s	Sampling period
T_{min}	Minimum time-constant of the linear section of the system
ω_S	Sampling frequency
z	z-transform operator
$G_{cd}(z)$	Transfer function of the series compensation controller stage in the discrete-time domain

1. Introduction

High quality performance of control systems can be achieved by applying the suggested cascade optimal digital compensation. It is implemented by employing a number of steps for the design of a proper digital compensator. The purpose of the compensator is to eliminate some properly selected poles of the system's transfer function. At the same time it introduces new dominant poles and a specifically designed amplification. As a result, the quality of the system's performance in terms of its transient response, stability and accuracy are considerably improved. The suggested technique of successive steps brings the system to its marginal state, further subjecting it to multi-stage phase-lead, phase-lag compensation and amplification. The continuous cascade compensator prototype is finally converted into its digital equivalent and implemented as a microcontroller compensator. The main purpose of the suggested method is the compensated control system to meet the ITAE criterion and accordingly, the following objectives [1]:

$\zeta = 0.707$; (PMO) $\leq$ 4%; $t_s/t_m \leq 1.4$; $e_{ss} \leq 1\%$ (type 0)

Phase-lead and phase-lag compensation technique is a well known mechanism for improving control systems' performance as demonstrated in considerable number of sources [1], [2], [3], [4]. The disadvantage of this method of compensation, as described in the sources, is that it only recommends the range of the compensator's frequencies and it depends on the designer's expertise to achieve the best performance of the compensated system. Further, the direct application of the compensation technique causes compromise with the system's gain.

Another method to meet the objectives of the ITAE criterion is to apply a PI or a PID controller to process control systems. This is a well known approach and it is also described in the sources mentioned above. Different methodologies are recommended for determination of the PI or PID controller constants where results are usually achieved with a lot of assumptions. Finally, the best system performance is proved to be accomplished by a procedure of manual MATLAB interaction tuning of the PI or PID controller constants [5].

The importance of the new controller design technique, presented by the author of this research, is that it is suggesting a straight forward and exact achievement of the ITAE criterion objectives. Further contribution of the suggested by the author technique is the conversion of the achieved controller from its continuous to its digital equivalent. In this way the compensation is implemented with the aid of microcontrollers that are programmed based of the difference equations, representing the digital transfer functions of the controller stages. The application of digital control is in accordance to the Euler's approximation [6], [7], [8]. It recommends that the sampling period T_s of the discrete system, should be within the range $T_s \leq (0.1T_{min}$ to $0.2T_{min})$, where T_{min} is the minimum time-constant of the continuous-time system or the analogue plant model prototype. Only then there will be a close match between the discrete and the continuous-time system performance and both, the optimal plant analogue prototype and its optimal digital equivalent are having exactly the same relative damping of $\zeta = 0.707$. If the Euler's approximation is applied, it is apparent that there is a complete match between the corresponding pole location on the s-plane and on the z-plane. Due to this conclusion, the controller stages are designed in the continuous-time domain and further converted into their discrete-time equivalents [9].

For the clarity of the presented research, this paper is organized in the following sequence. Initially, the compensation design for a system Type 0 is described for the cases of considerable difference and insignificant difference between dominant and insignificant system poles. With the aid of three successive steps the system's performance is preliminary evaluated. Further, the implementation of five successive rules are bringing the system's performance to perfection, satisfying the ITAE criterion objectives. This is followed by the application of the compensation technique to a system Type 1. Finally, a pseudo code technique is applied for describing the different system cases with the aid of a flowchart, in this way clarifying the paths and steps that are to be followed for the design of the compensation.

2. Compensator Design for a System Type 0

Case 1: Considerable Difference between Dominant and Insignificant Poles

The compensation design can be demonstrated for a case of a **cruise control system** [10] with a transfer function:

$$G_{P1}(s) = \frac{K'}{(1+T_1 s)(1+T_2 s)(1+T_3 s)} = \\ = \frac{10}{(1+0.1s)(1+0.2s)(1+s)} = \\ = \frac{500}{s^3+16s^2+65s+50} = \frac{K}{s^3+16s^2+65s+50} \quad (1)$$

Step 1: Evaluation of the Original Control System

The system's performance is unacceptable due to large oscillations as seen from Figure 1. The system's transient response is achieved by applying the following MATLAB code:

```
>> Gp1=tf([0 500],[1 16 65 50])
>> Gfb1=feedback(Gp1,1)
>> step(Gfb1)
```

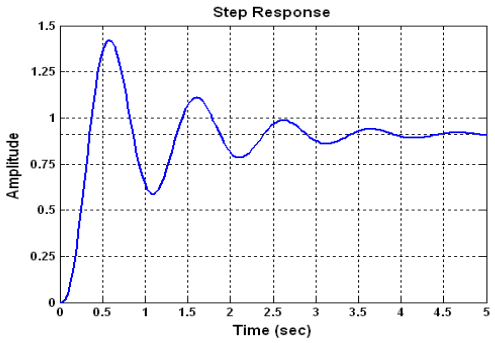

Figure 1: Transient Response of the Original Control System

Step 2: Determination of the Marginal System Gain

To apply the suggested compensation technique, the system initially has to be brought to its marginal state by tuning its original gain K'. The critical value of K' is achieved by means of applying the proposed by the author, in some of his previous publications, method of Advanced D-Partitioning [11], [12], [13].

To apply this method, the characteristic equation of the system (2) is derived from Equation (1), considering the system's gain value $K' = 0.02K$ as unknown.

$$G_P(s) = s^3 + 16s^2 + 65s + 50 + K \quad (2)$$

From Equation (2) the unknown value of K can be presented as follows:

$$K = -s^3 - 16s^2 - 65s - 50 \quad (3)$$

The D-partitioning curve in terms of the variable parameter K can be plotted in the complex plane within the frequency range $-\infty \leq \omega \leq +\infty$ facilitated by MATLAB the "nyquist" m-code, as seen in Figure 2.

```
>> K=tf([-1 -16 -65 -50],[0 1])
Transfer function:
-s^3 - 16 s^2 - 65 s - 50
>> nyquist(K)
```

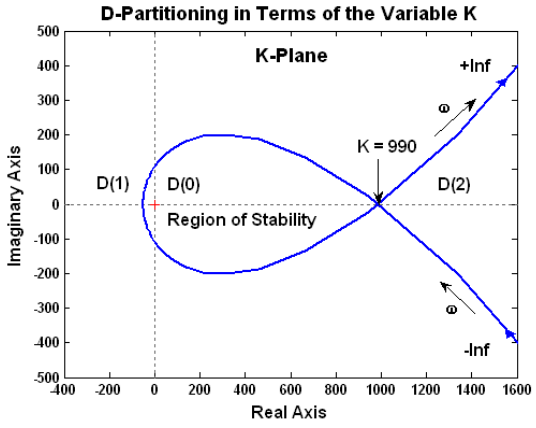

Figure 2: D-Partitioning Facilitated by the "nyquist" m-code

To avoid any misinterpretation of the D-Partitioning procedure, the "nyquist" m-code can be modified into a "dpartition" m-code with the aid of the MATLAB Editor and a proper formatting.

It is seen that the D-partitioning determines three regions on the K-plane: D(0), D(1) and D(2). Applying the Advanced D-Partitioning method, only D(0) is the region of stability, being always on the left-hand side of the curve for the frequency range from $-\infty$ to $+\infty$ [11], [12].

At $K = 990$, the system is marginal and the system's gain becomes $K' = 0.02K = 0.02\times990 = 19.8$.

Comparison between the original and the marginal system transient responses is shown in Figure 3.

```
>> Gp1=tf([0 500],[1 16 65 50])
>> Gfb1=feedback(Gp1,1)
>> Gp2=tf([0 990],[1 16 65 50])
>> Gfb2=feedback(Gp2,1)
>> step(Gfb1,Gfb2)
```

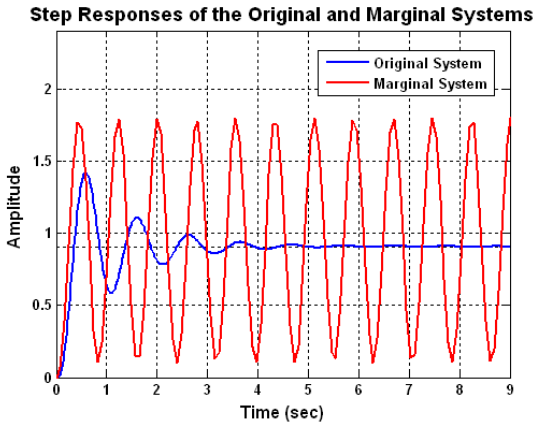

Figure 3: Comparison between the Original and the Marginal Linear Prototype Systems' Transient Responses

Considering Equation (1), the transfer function of the marginal control system is presented as:

$$G_{P2}(s) = \frac{19.8}{(1+0.1s)(1+0.2s)(1+s)} \tag{4}$$

Step 3: Optimization of ζ, t_s/t_m and PMO

Initially, the cascade compensator is designed as a continuous prototype and further it is converted into its digital equivalent. The following rules are applied:

Rule 1: To optimize ζ, t_s/t_m and the PMO of a Type 0 marginal closed-loop system, a cascade multi-stage compensation with factors of $\alpha_{1,2,3,\ldots} = 10$ is applied for a zero-pole cancellation.

This rule is considered from the graphical relationship of Figure 4 [13], [14].

The number of the compensating stages N is to be one less than the order of the open-loop system, i.e. N = n + m – 1.

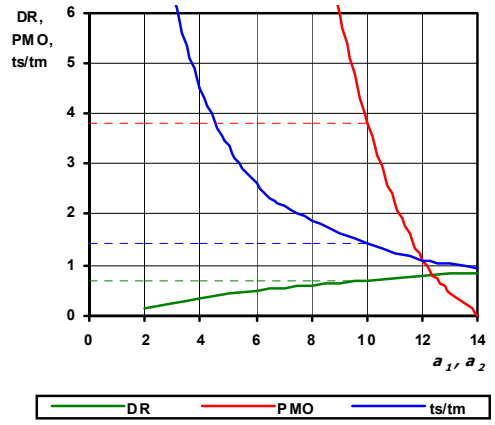

Figure 4: Determination of the Optimum Values of α_1 and α_2

The most dominant pole of the open-loop system should be left uncompensated. Since the plant transfer function from Equation (1) is of a third order, according to Rule 1, the multi-stage lead section of the compensator continuous prototype should have a transfer function:

$$G_c'(s) = \frac{(1+\alpha_1 T_1 s)(1+\alpha_2 T_2 s)}{\alpha_1 \alpha_2 (1+T_1 s)(1+T_2 s)} = \frac{(1+0.1s)(1+0.2s)}{100(1+0.01s)(1+0.02s)} \tag{5}$$

Rule 2: The current gain is maintained by amplification equal to the product $\alpha_1\alpha_2\alpha_3\ldots$[13], [14].

$$G_c''(s) = \alpha_1 \alpha_2 = 10\times10 = 100 \tag{6}$$

Rule 3: To optimize a marginal closed-loop system, single-stage section of the continuous prototype lag compensator with factor $\beta = 10$ is to be applied for a zero-pole cancellation of the uncompensated most dominant pole of the open-loop system.

To optimize the steady-state error e_{ss} the current gain should be increased by the factor $\gamma = 10$ (proved from Figure 5 [13], [14]. Both relationships shown in Figure 4 and Figure 5 are achieved by tracking procedures.

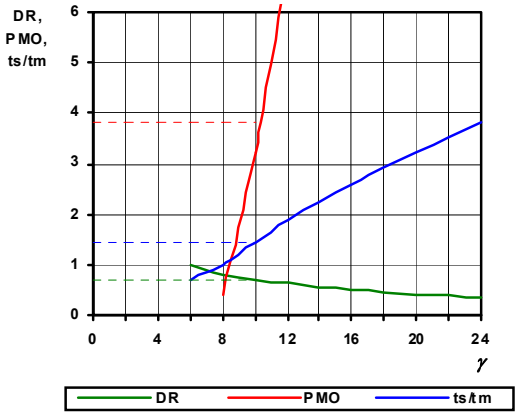

Figure 5: Determination of Optimum Value of γ

The most significant pole in Equation (1) is $p_3 = -1$. Applying Rule 2, the section of the lag compensation and amplification is presented by:

$$G_c'''(s) = \frac{\gamma(1+T_3 s)}{(1+\beta T_3 s)} = \frac{10(1+s)}{(1+10s)} \quad (7)$$

The transfer function of the full compensator is the product of the transfer functions of the three sections:

$$G_c(s) = G_c'(s) \times G_c''(s) \times G_c'''(s) = \\ = \frac{10(1+0.1s)(1+0.2s)(1+s)}{(1+0.01s)(1+0.02s)(1+10s)} \quad (8)$$

Applying the full compensation, taking into account equations (4) and (8), the transfer function of the open-loop system becomes:

$$G(s) = G_c(s) \times G_p(s) = \\ = \frac{100}{(1+0.01s)(1+0.02s)(1+10s)} \\ = \frac{100}{0.002s^3 + 0.3002s^2 + 10.03s + 1} \quad (9)$$

Comparison between the transient responses of the original, the marginal and the compensated system, as shown in Figure 6, is achieved by the code:

```
>> Gp1=tf([0 500],[1 16 65 50])
>> Gfb1=feedback(Gp1,1)
Transfer function:
        500
-------------------------
s^3 + 16 s^2 + 65 s + 550
>> Gp2=tf([0 990],[1 16 65 50])
>> Gfb2=feedback(Gp2,1)
Transfer function:
        990
-------------------------
s^3 + 16 s^2 + 65 s + 1040
>> Gp3=tf([0 100],[0.002 0.3002 10.03 1])
>> Gfb3=feedback(Gp3,1)
Transfer function:
          100
-------------------------------------
0.002 s^3 + 0.3002 s^2 + 10.03 s + 101
>> step(Gfb1,Gfb2,Gfb3)
```

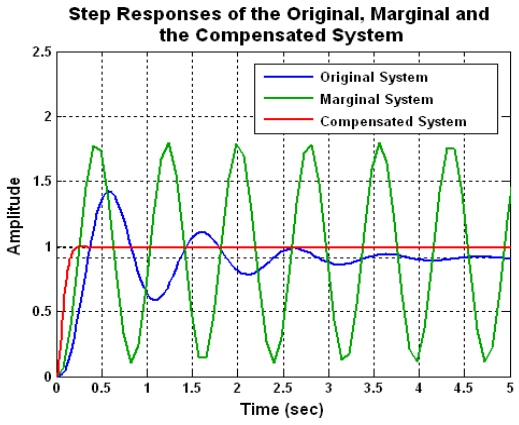

Figure 6: Comparison between the Transient Responses of the Original, Marginal and Compensated Linear Prototype Systems

The Bode diagram of the compensated system is plotted by applying the code:

```
>> Gp3=tf([0 100],[0.002 0.3002 10.03 1])
>> margin (Gp3)
```

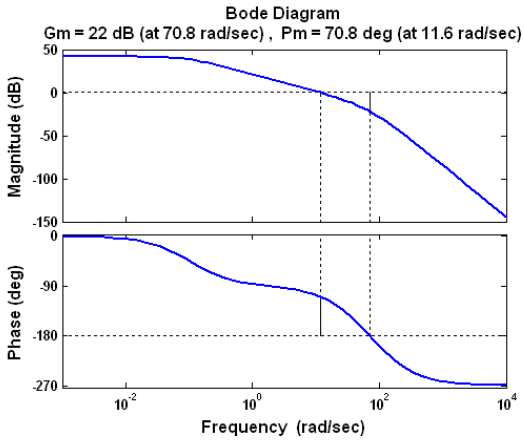

Figure 7: Bode Diagrams of the Compensated System Proving Phase Margin PM = 70.8 and Damping $\zeta \approx 0.707$

The system performance after the compensation, seen from the transient response in Figure 6 and the Bode diagram in Figure 7, demonstrates the achievement of optimal performance [1], [2], [14].

Step 4: Conversion of the Continuous Prototype Compensated System into its Digital Equivalent.

In order to apply digital compensation control, in accordance to the Euler's approximation [15] the sampling period T_s of the discrete system, should be within the range $T_s \leq (0.1T_{min}$ to $0.2T_{min})$, where T_{min} is the minimum time-constant of the continuous-time system.

By applying the Euler's approximation, a close match is expected between the discrete and the continuous-time system performance. For the case under discussion, the plant's minimum time constant is $T_{min} = 0.1$sec and the sampling period is chosen as $T_s = 0.01$ sec, satisfying the condition $T_s \leq 0.1T_{min}$. When analysis is applied in the discrete-time domain, the considered frequency variation is within the range $\omega = \pm \omega_s/2 = \pm 2\pi/2T_s$ [6], [16].

The analysis in the discrete-time domain is applied with the aid of the Bilinear Tustin Transform [16], [17] that is a first-order approximation of the natural logarithm function, being an exact mapping of the z-plane to the s-plane and vice versa. It maps positions from the $j\omega$ axis in the s-plane to the unit circle $|z| = 1$ in the z-plane. The Bilinear Tustin approximation and its inverse are presented as [16]:

$$z = e^{sT_s} = \frac{e^{sT_s/2}}{e^{-sT_s/2}} \approx \frac{1+sT_s/2}{1-sT_s/2}; \; s = \frac{1}{T_s}\ln(z) \approx \frac{2}{T_s}\frac{z-1}{z+1} \quad (10)$$

To employ the Bilinear Tustin Transform, the MATLAB *'tustin'* code is to be applied, performing the transform of the continuous-time to discrete-time system equivalents. The results demonstrated in Figure 6 and Figure 7 can be compared with the results after converting the analogue system model prototype into its digital equivalent:

```
>>  Gp1=tf([0 500],[1 16 65 50])
>> Gfb1=feedback(Gp1,1)
>> Gp3=tf([0 100],[0.002 0.3002 10.03 1])
>> Gfb1d = c2d(Gfb1,0.01,'tustin')
Transfer function:
5.778e-005 z^3 + 0.0001733 z^2 + 0.0001733 z + 5.778e-005
-----------------------------------------------------
      z^3 - 2.846 z^2 + 2.698 z - 0.852
Sampling time: 0.01
>> Gfb3d = c2d(Gfb3,0.01,'tustin')
Transfer function:
0.003321 z^3 + 0.009962 z^2 + 0.009962 z + 0.003321
---------------------------------------------------
     z^3 - 1.916 z^2 + 1.139 z - 0.1958
Sampling time: 0.01
>> step(Gfb1d,Gfb3d)
```

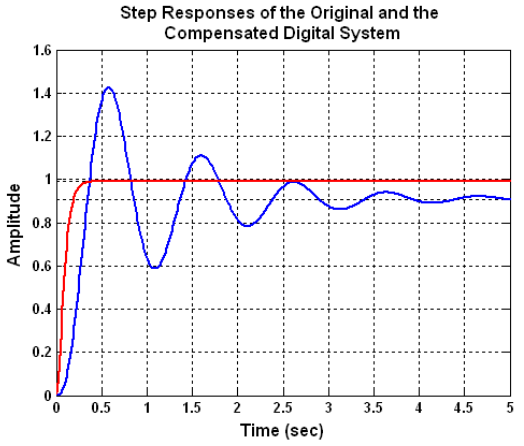

Figure 8: Comparison between the Transient Responses of the Original and Compensated Digital Systems

The Bode diagram of the compensated digital system is plotted by applying the code:

```
>> Gp3=tf([0 100],[0.002 0.3002 10.03 1])
>>  Gp3d = c2d(Gp3,0.01,tustin')
Transfer function:
0.003332 z^3 + 0.009995 z^2 + 0.009995 z + 0.003332
---------------------------------------------------
     z^3 - 1.932 z^2 + 1.132 z - 0.1998
Sampling time: 0.01
 >> margin (Gp3d)
```

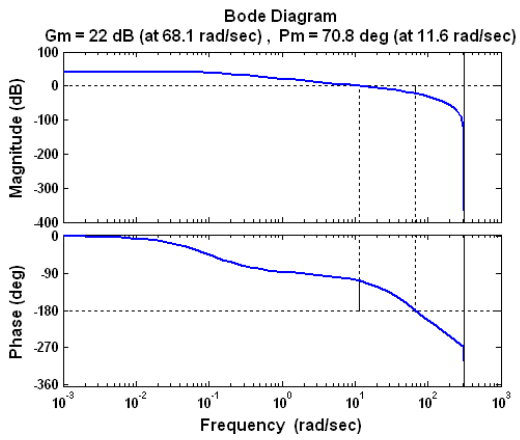

Figure 9: Bode Diagrams of the Digital Compensated System Proving Phase Margin PM = 70.8 and Damping $\zeta \approx 0.707$

The results obtained from Figure 8 and Figure 9, compared with the results from Figure 6 and Figure 7, prove the close match between the performance of the continuous-time model prototype and the digital model of the system (PM = 70.8 and $\zeta \approx 0.707$).

The performance specifications of the compensated system, determined from the transient response and the Bode diagram shown in Figure 8 and Figure 9, are compared with the objectives for optimal performance.

Table 1

Objectives and Real Results for Case 1

Specifications	Objectives	Real Results	Consideration
ζ	= 0.707	= 0.707	Matching
PMO	$\leq$ 4%	= 2.8%	Better
$t_{s(1\%)}/t_m$	$\leq$ 1.49	= 1.25	Better
$e_{ss}(t)$	< 1%	= 0.06%	Better

From the graphs at Figure 8 and Figure 9 and from the summary in Table 1, it is seen that the transient response of the compensated system in terms of relative damping ratio ζ, percent maximum overshoot (PMO), time ratio $t_{s(1\%)}/t_m$ and steady-state error $e_{ss}(t)$ is either matching or it is better than the one of the set objective.

Step 5: Design of a Digital Compensation Controller based on a Microcontroller (Case 1).

The design of a digital compensation controller founded on its analogue prototype is realized again by applying the Tustin bilinear transform [16], [17]. From the Equation (8), the transfer function of the modified compensation controller stage can be presented as:

$$G_c(s) = \frac{10(1+0.1s)(1+0.2s)(1+s)}{(1+0.01s)(1+0.02s)(1+10s)} = \\ = \frac{2s^3 + 32s^2 + 130s + 100}{0.02s^3 + 3.002s^2 + 100.3s + 10} \quad (11)$$

The digital equivalent of the series compensator controller stage [16], [17] is realized by the code:

```
>> Gc=tf([2 32 130 100],[0.02 3.002 100.3 10])
>> Gcd = c2d(Gc,0.1,'tustin')
Transfer function:
9.328 z^3 - 17.15 z^2 + 9.743 z - 1.688
---------------------------------------
z^3 + 0.1052 z^2 - 0.7986 z - 0.2829
Sampling time: 0.1
```

Following the code result, the transfer function of the series compensation controller stage in the discrete-time domain is as follows:

$$G_{cd}(z) = \frac{9.328z^3 - 17.15z^2 + 9.743z - 1.688}{z^3 + 0.1052z^2 - 0.7986z - 0.2829} = \frac{Y(z)}{X(z)} \quad (12)$$

To enable the implementation of a microcontroller that is connected in cascade with the original plant, the transfer function of the series digital robust control stage is represented by the following difference equation [18]:

$$y(kT) = 0.1052\,y\left[(k-1)T\right] - 0.7986\,y\left[(k-2)T\right] + \\ -0.2829\,y\left[(k-3)T\right] + \\ +9.328\,x(kT) - 17.15\,x\left[(k-1)T\right] + \\ +9.743\,x\left[(k-2)T\right] - 1.688\,x\left[(k-3)T\right] \quad (13)$$

Case 2: Insignificant Difference between Dominant and Insignificant Poles

Rule 4: If the most significant pole of the open-loop system has a real part close in value to that of an insignificant pole, Rule 3 is modified to Rule 4, where successive two-stage lag compensation with factors $\beta_1 = \beta_2$ and a factor δ should be applied.

The values of the factors β_1 and β_2 at Rule 4 are chosen by the same considerations as in Rule 2. The value of the factor δ is varied by a tracking procedure on the transient response, searching for the optimum performance of the compensated system. It is seen from Figure 10 that the set of objectives can be met if the factor $\delta = 80$ [13], [18].

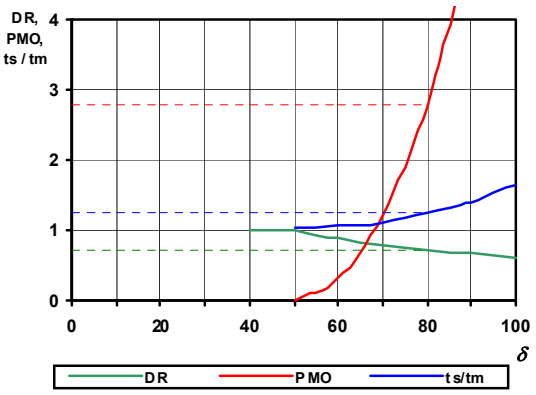

Figure 10: Determination of Optimum Value of δ

Rule 4 can be illustrated for a system Type 0 [19] of an **armature control dc motor and a type driving mechanism** with original gain $K = 10$. Applying the D-partitioning technique it is brought to its marginal state, where its gain becomes $K = 20$, as demonstrated below:

$$G_{P3}(s) = \frac{20}{(1+0.01s)(1+0.02s)(1+0.1s)} \quad (14)$$

The real part of the most significant pole is $p_3 = -10$ and it is only 5 times smaller than the real part of the one of the insignificant poles $p_1 = -50$.

Again, in accordance to Rule 1, a two-stage lead compensation and attenuation is applied, where the factors are $\alpha_1 = \alpha_2 = 10$. Following Rule 2, the gain is maintained by amplification equal to the product $\alpha_1\alpha_2$. Further, following Rule 4, a two-stage lag compensation with factors $\beta_1 = \beta_2 = 10$ and a factor amplification $\delta = 80$ is suggested. Using a related sequence and applying Equation (5), the two-stage lead stage is presented by:

$$G_c'(s) = \frac{(1+\alpha_1 T_1 s)(1+\alpha_2 T_2 s)}{\alpha_1\alpha_2(1+T_1 s)(1+T_2 s)} = \\ = \frac{(1+0.01s)(1+0.02s)}{100(1+0.001s)(1+0.002)} \quad (15)$$

Applying Rule 2, the second compensation section is achieving the amplification:

$$G_c''(s) = \alpha_1\alpha_2 = 10\times 10 = 100 \quad (16)$$

Applying Rule 4, the two-stage lag compensation and amplification is presented by:

$$G_c'''(s) = \frac{\delta(1+T_3 s)(1+T_4 s)}{(1+\beta_1 T_3 s)(1+\beta_2 T_4 s)} = \frac{80(1+0.1s)(1+s)}{(1+s)(1+10s)} \quad (17)$$

The transfer function of the complete compensator as a product of the three sections is:

$$G_c(s) = G_c'(s)\times G_c''(s)\times G_c'''(s) = \\ = \frac{80(1+0.01s)(1+0.02s)(1+0.1s)}{(1+0.001s)(1+0.002s)(1+10s)} \quad (18)$$

After applying the full compensation, considering Equations (14) and (18), the analogue prototype of the transfer function of the open-loop compensated system becomes:

$$G(s) = G_c(s)\times G_p(s) = \\ = \frac{1600}{(1+0.001s)(1+0.002s)(1+10s)} \quad (19)$$

In the same way the Bilinear Tustin Transform is applied, converting the continuous-time system prototype into its digital equivalent. The system's transient response before and after compensation is shown in Figure 11 and is obtained by the following code:

```
>> Gp1=500000/(s+10)/(s+50)/(s+100)
>> Gpfb1=feedback(Gp1,1)
>> G=80000000/(s+0.1)/(s+500)/(s+1000)
>> Gfb=feedback(G,1)
>> Gpfb1d = c2d(Gpfb1,0.002,'tustin')
>> Gfbd = c2d(Gfb,0.002,'tustin')
>> step(Gpfb1d,Gfbd)
```

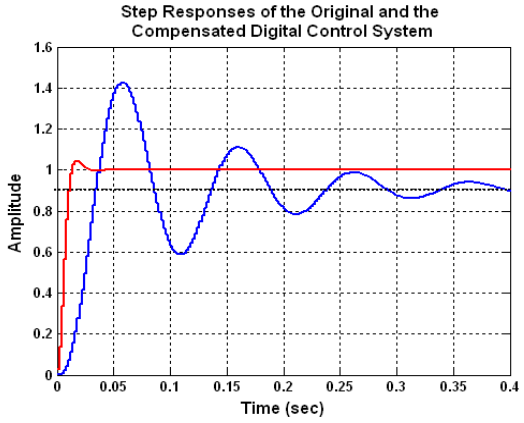

Figure 11: Comparison between the Transient Responses of the Original and Compensated Digital System (Case 2)

The Bode diagram of the compensated digital system is shown at Figure 11 and plotted by applying the code:

```
>> G=80000000/(s+0.1)/(s+500)/(s+1000)
>> Gd = c2d(G,0.002,'tustin')
Zero/pole/gain:
 0.026664 (z+1)^3
-----------------
z (z-1) (z-0.3333)
Sampling time: 0.002
```

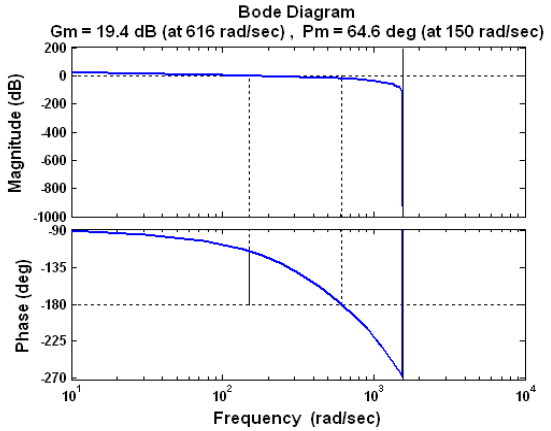

Figure 12: Bode Diagrams of the Digital Compensated System Proving Phase Margin PM = 64.6 and Damping $\zeta \approx 0.646$

From the summary in Table 2, it is obvious that the objectives are met. Again, the real results for the compensated control system are either close or better than the set specifications.

Table 2

Objectives and Real Results for Case 2

Specifications	Objectives	Real Results	Consideration
ζ	= 0.707	= 0.646	Close
PMO	$\leq$ 4%	= 2.8%	Better
$t_{s(1\%)}/t_m$	$\leq$ 1.49	= 1.25	Better
$e_{ss}(t)$	< 1%	= 0.06%	Better

Step 5: Design of a Digital Compensation Controller based on a Microcontroller (Case 2).

The digital equivalent of the series compensator controller stage can be realized in a similar procedure, like the one implemented for example of Case 1. The transfer function compensation controller stage sown in equation (18) is modified and can be presented in the following format:

$$G_c(s) = \frac{80(1+0.01s)(1+0.02s)(1+0.1s)}{(1+0.001s)(1+0.002s)(1+10s)} = \\ = \frac{0.0016s^3 + 0.256s^2 + 10.4s + 80}{0.00002s^3 + 0.030002s^2 + 10.003s + 1} \quad (20)$$

Considering the equation (20), the digital equivalent of the series compensator controller stage is realized by the code:

```
>> Gc=tf([0.0016 0.256 10.4 80],[0.00002 0.030002 10.003 1])
Transfer function:
0.0016 s^3 + 0.256 s^2 + 10.4 s + 80
-----------------------------------
 2e-005 s^3 + 0.03 s^2 + 10 s + 1
>> Gcd = c2d(Gc,0.01,'tustin')
Transfer function:
1.891 z^3 + 1.441 z^2 - 0.1501 z - 0.1801
-----------------------------------------
 z^3 + 0.8938 z^2 - 0.9782 z - 0.8781
Sampling time: 0.01
```

Following the code result, the transfer function of the series compensation controller stage in the discrete-time domain is as follows:

$$G_{cd}(z) = \frac{1.891z^3 + 1.441z^2 - 0.1501z - 0.1801}{z^3 + 0.8938z^2 - 0.9782z - 0.8781} = \frac{Y(z)}{X(z)} \quad (21)$$

Taking into accounting equation (21), the transfer function of the series digital robust control stage is represented by the following difference equation (22). A microcontroller, connected in cascade with the original plant, can be programmed in accordance with this difference equation [18], [20]:

$$\begin{aligned} y(kT) = {} & 0.8938\,y[(k-1)T] - 0.9782\,y[(k-2)T] + \\ & - 0.8781\,y[(k-3)T] + \\ & + 1.891\,x(kT) + 1.441\,x[(k-1)T] + \\ & - 0.1501\,x[(k-2)T] - 0.1801\,x[(k-3)T] \end{aligned} \quad (22)$$

3. Compensator Design for a System Type 1

The compensation technique for a **light tracking system** with a transfer function of Type 1 can be demonstrated with the aid of the following transfer function [21], [22]:

$$G_{P4}(s) = \frac{K'}{s(1+T_1 s)(1+T_2 s)} = \frac{50}{s(1+0.02s)(1+0.05s)} = \\ = \frac{500}{s^3 + 7s^2 + 100s} = \frac{K}{s^3 + 7s^2 + 100s} \quad (23)$$

Step 1: Evaluation of the Original Control System

The demonstration of the system's transient response is achieved by applying the following code:

```
>>Gp4=tf([0 500],[1 7 100 0])
Transfer function:
      500
 ------------------
 s^3 + 7 s^2 + 100 s
>> Gfb4=feedback(Gp4,1)
>> step(Gfb4)
```

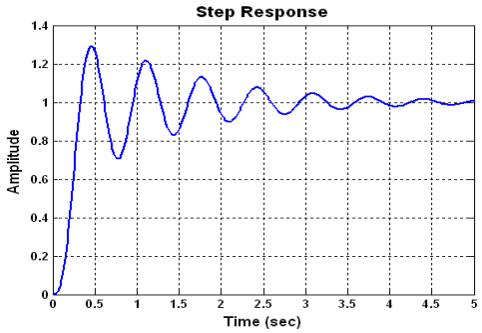

Figure 13: Transient Response of the Original System Type *1*

Step 2: Determination of the Marginal System Gain

The critical marginal value of the unknown parameter K is achieved by means of applying the method of Advanced D-Partitioning. From equation (23), the characteristic equation of the system is obtained as:

$$G_P(s) = s^3 + 7s^2 + 100s + K \tag{24}$$

Reflecting on equation (24) the unknown value of K can be presented as follows:

$$K = -s^3 - 7s^2 - 100s \tag{25}$$

The D-partitioning curve in terms of the variable parameter K can be plotted in the complex plane within the frequency range $-\infty \le \omega \le +\infty$ facilitated by the following code and seen in Figure 14.

```
>> K=tf([-1 -7 -100 0],[0 1])
Transfer function:
-s^3 - 7 s^2 - 100 s
>> nyquist(K)
```

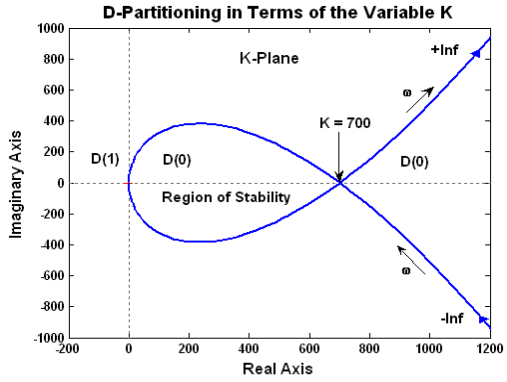

Figure 14: D-Partitioning in Terms of the Parameter K

The D-partitioning determines three regions on the K-plane: D(0), D(1) and D(2). Only D(0) is the region of stability, being the one, always on the left-hand side of the curve for a frequency variation from $-\infty$ to $+\infty$.

At $K = 700$, the system is marginal and the system's gain becomes $K' = 0.1K = 0.1\times700 = 70$.

Then equation (23) of the plant transfer function of Type 1 is modified to its marginal case as follows:

$$G_{P4}(s) = \frac{K'}{s(1+T_1 s)(1+T_2 s)} = \frac{70}{s(1+0.02s)(1+0.05s)} \tag{26}$$

Step 3: Optimization of ζ , t_s / t_m and PMO

For optimization of a marginal closed-loop system of Type 1, Rule 1 is used in the same manner, while Rule 2 is modified to Rule 5 and Rule 3 is ignored.

Rule 1: To optimize ζ, t_s/t_m and the PMO of a Type 1 marginal closed-loop system, a cascade multi-stage lead compensation with factors of $\alpha_{1,2,3,\ldots}=10$ should be applied for a zero-pole cancellation. The number of the compensating stages N should be one less than the order of the open-loop system $N = n + m - 1$.

Rule 5: The pure integration or the most significant pole of the open-loop system should be left uncompensated. The existing system gain should be maintained by amplification equal to the product $\varepsilon\alpha_1\alpha_2\alpha_3\ldots$, where the compensation amplification factor is $\varepsilon = (0.1 \text{ to } 1.27)$.

To keep $\zeta = 0.707$, when the ratio of the less significant to the most significant pole of the plant transfer function, $r = p_1/p_2$, varies from 50 to 1, the value of ε may vary from 0.1 to 1.27. The case $r = 2.5$, $\varepsilon = 1$ can be identified as shown in Figure 15 [23], [24], [25].

If the ratio is $r = 2.5$, as in the discussed case, then $\varepsilon = 1$. If $r < 2.5$, ε is within the limits $\varepsilon = (1 \text{ to } 1.27)$. If $r > 2.5$, then ε should be within the limits $\varepsilon = (0.1 \text{ to } 1)$.

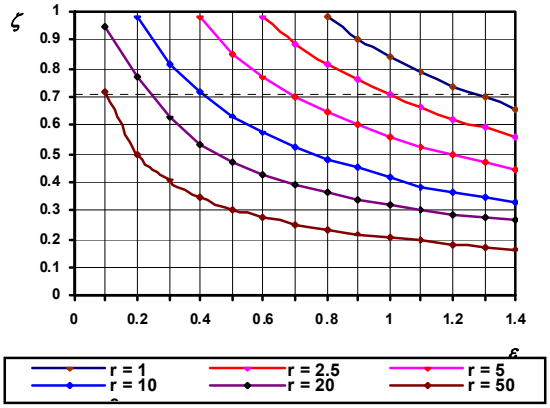

Figure 15: Relationship between the Damping Ratio ζ and the Factor ε for Different Poles Ratios $r = p_1/p_2$

For the plant with the transfer function represented by Equation (26), a two-stage lead compensation and attenuation is applied. The poles $p_1 = -50$ and $p_2 = -20$ are cancelled and amplification factors $\alpha_1 = \alpha_2 = 10$ and $\varepsilon = 1$ are used.

By applying Rule 1 and using a related sequence, the two-stage lead stage is presented by:

$$G_c'(s) = \frac{(1+\alpha_1 T_1 s)(1+\alpha_2 T_2 s)}{\alpha_1 \alpha_2 (1+T_1 s)(1+T_2 s)} = \frac{(1+0.02s)(1+0.05s)}{100(1+0.002s)(1+0.005)} \tag{27}$$

Further from Rule 5:

$$G_c''(s) = \varepsilon\alpha_1\alpha_2 = 1\times10\times10 = 100 \tag{28}$$

The transfer function of the complete compensator as a product of the three sections is:

$$G_c(s) = G_c'(s)\times G_c''(s) = \frac{100(1+0.02s)(1+0.05s)}{100(1+0.002s)(1+0.005s)} = \frac{(1+0.02s)(1+0.05s)}{(1+0.002s)(1+0.005s)} \tag{29}$$

By applying the full compensation, considering Equations (26) and (29), the continuous prototype of the transfer function of the open-loop compensated system becomes:

$$G(s) = G_c(s) \times G_{p4}(s) = \\ = \frac{70}{s(1+0.002s)(1+0.005s)} \quad (30)$$

Step 4: Conversion of the Continuous Prototype Compensated System into its Digital Equivalent.

The transient responses of the closed-loop digital control system before and after the compensation are shown in Figure 16 and are obtained by the code:

```
>> Gp=50000/(s+50)/(s+20)/(s+0)
>> Gpfbd = c2d(Gpfb,0.004,'tustin')
>> G=7000000/(s+500)/(s+200)/(s+0)
>> Gpfbd = c2d(Gpfb,0.002,'tustin')
>> step(Gpfbd,Gfbd)
```

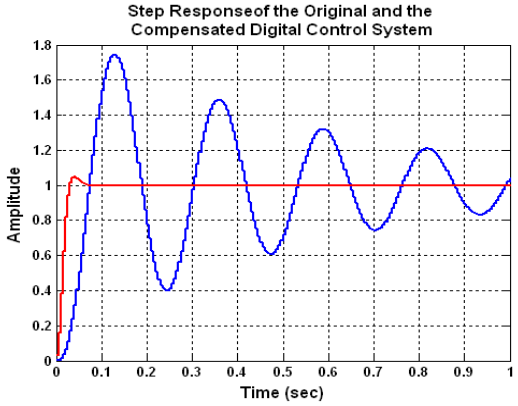

Figure 16: Comparison between the Transient Responses of the Original and Compensated Digital System Type 1

The Bode diagrams, after applying the compensation technique, are achieved by the code as shown below and are presented in Figure 17.

```
>> Gpd=c2d(Gp,0.005,'tustin')
>>Gd=c2d(G,0.005,'tustin')
>> margin(Gd)
```

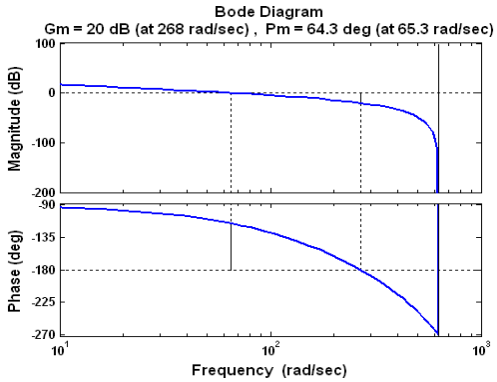

Figure 17: Bode Diagrams of the Digital Compensated System Proving Phase Margin PM = 64.3 and Damping $\zeta \approx 0.643$

Comparison between the results and the objectives for optimal performance is summarized in Table 3. It is seen from Figure 16, Figure 17 and Table 3 that the results after the digital compensation are better or a close match with the objectives.

Table 3

Objectives and Real Results for Case 3

Specifications	Objectives	Real Results	Consideration
ζ	= 0.707	= 0.643	Close
PMO	≤ 4%	= 3.3%	Better
$t_{s(1\%)}/t_m$	≤ 1.49	= 1.4	Better
$e_{ss}(t)$	= 0%	= 0%	Matching

Step 5: Design of a Digital Compensation Controller based on a Microcontroller (Case 3).

If considering Equation (29), the transfer function of the modified compensation controller stage can be presented as:

$$G_c(s) = \frac{(1+0.02s)(1+0.05s)}{(1+0.002s)(1+0.005s)} = \\ = \frac{0.001s^2 + 0.07s + 1}{0.00001s^2 + 0.007 + 1} \quad (31)$$

Further, the digital equivalent of the compensator controller stage is realized by the code:

```
>> Gc=tf([0.001 0.07 1],[0.00001 0.007 1])
Transfer function:
 0.001 s^2 + 0.07 s + 1
-----------------------
1e-005 s^2 + 0.007 s + 1
>> Gcd = c2d(Gc,0.001,'tustin')
Transfer function:
75.29 z^2 - 145.4 z + 70.2
--------------------------
 z^2 - 1.418 z + 0.4909
Sampling time: 0.001
```

Then, the transfer function of the series controller stage in the discrete-time domain is as follows:

$$G_{cd}(z) = \frac{75.29z^2 - 145.4z + 70.2}{z^2 - 1.418z + 0.4909} = \frac{Y(z)}{X(z)} \quad (32)$$

Similarly to the other cases, a microcontroller can be connected in cascade with the original plant. To program the microcontroller, the transfer function of the series digital robust control stage is represented by the following difference equation [26], [27], [28]:

$$y(kT) = -1.418\,y[(k-1)T] + 0.4909\,y[(k-2)T] + \\ + 75.29\,x(kT) + \\ - 145.4\,x[(k-1)T] + 70.2\,x[(k-2)T] \quad (33)$$

Figure 18 demonstrates the analogue prototype of the compensated system.

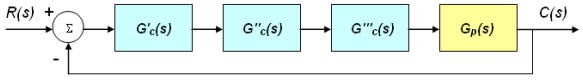

Figure 18: Block Diagram of the Analogue Prototype Compensated System

In Figure 19, the continuous model is converted into its digital equivalent by introducing the compensating microcontroller.

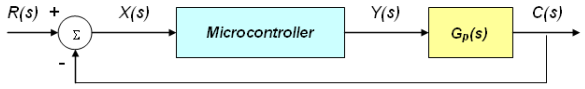

Figure 19: Block Diagram of the Digital Compensated System

4. Flowchart Diagram of the Analysis and Design Procedure Sequence

The sequence of the analysis and the design procedure are described by the following flowchart diagram [29].

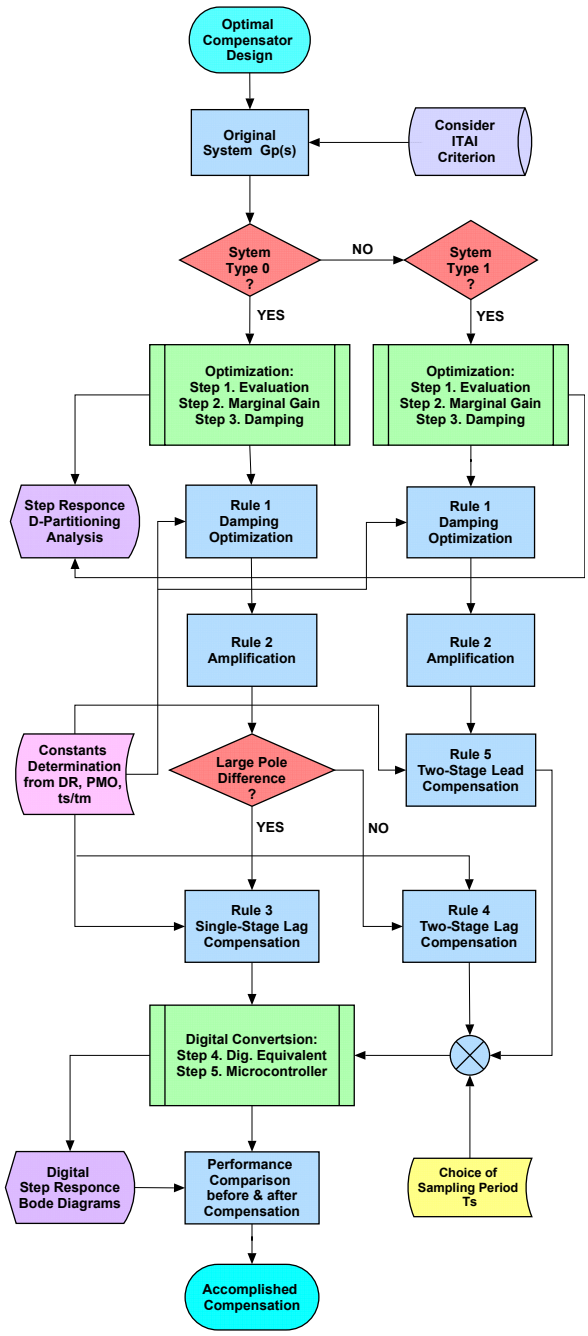

Figure 20: Flowchart Diagram of the Analysis and Compensator Design Procedure Sequence

This section describes the interactive procedure sequence [30], [31] for the analysis and design of the digital optimal compensation of the process control system.

The system identification is an important element of any process of analysis. The dynamics of the plant process control system is described by a differential equation and further its transfer function $G_P(s)$ can be derived. The ITAE criterion is considered for the design of the optimal compensator.

Further, the system is identified as Type 0 or Type 1. For any one of the cases evaluation of the system is performed in terms of transient response, marginal gain and relative damping. The design procedure sequence applying Rule 1 and Rule 2 follows in terms of relative damping optimization and proper amplification.

The constants α, γ, δ and ε are determined from their graphical relationships with the DR, PMO and t_s/t_m. These constants are further used for the implementation of Rule 1, Rule 3, Rule 4 and Rule 5.

The results are presented graphically after the initial system optimization, applying Step 1, Step 2 and Step 3 and displaying the original system transient response and gain margin original with the aid of the D-partitioning stability analysis.

If the system is Type 0, it is examined in terms of the difference between its dominant and its insignificant poles. If the difference is large, single stage lag compensation is applied. If the difference is insignificant, two-stage lag compensation is applied. For a system of Type 1, two-stage lead compensation is applied.

Finally, considering the Euler's approximation for choice of the proper sampling period T_s and applying the Bilinear Tustin Transform, digital conversion from the continuous-time presentation into the digital equivalent is performed by applying Step 4 and Step 5.

Taking into account the compensator's digital transfer function, its corresponding difference equation is derived based on which a microcontroller can be programmed to operate as a digital optimal compensator.

The results after the digital conversion are presented graphically in the digital time-domain in terms of the system's transient response and Bode diagram.

Comparison is completed for the system's performance before and after applying of the digital compensator and it is observed that an optimal compensation is accomplished.

5. Conclusion

The originality of the suggested technique of multi-stage compensation is based on the statement of a number of rules, which are applied in a predetermined sequence to some known theoretical procedures, like lead-lag compensation and zero-pole cancellation.

By analyzing, combining and applying these rules to control systems of different nature, some new ideas are developed, bringing exceptional final results of the system's performance.

The analogue compensation equipment consists of three major parts, facilitating the initial stage of the design.

The analogue lead compensator section eliminates all insignificant poles of the original plant transfer function and introduces new properly designed dominant poles, improving the transient response and especially the relative damping ratio of the system.

The amplifying section of the compensator reduces considerably the steady-state error.

The analogue lag compensator section eliminates the most significant pole of the original plant transfer function and improves further the transient response.

To upgrade further the compensator equipment, its analogue continuous transfer function is converted to its digital equivalent. This conversion is taking into account the Euler's approximation and is achieved by applying the Bilinear Tustin Transform, considered as one of the most accurate techniques.

The excellent final results, observed from the digital system performance, prove once again the perfect match between the continuous compensator and its digital equivalent, due to the application of the Euler's technique.

Difference equations are derived based on the digital equivalents of the compensators transfer functions. Microcontroller connected in cascade with the original plant can be programmed, based on the difference equation, reflecting the operation of the digital compensator.

The latest manufactured microcontrollers offer very high operating frequencies that can handle successfully the operation of each one of the discussed in this research control systems. For example the TMS320F2837xS is a powerful 32-bit floating-point microcontroller designed for advanced closed-loop control applications that provides 200 MHz of signal processing performance [32] and can be used for each one of the considered cases.

There is significant number of advantages associated with the digital control systems, compared with the continuous control systems. Due to this reason, the choice of compensation design strategy, resulting in the implementation of microcontrollers, is the better and preferable option and can be applied for any process control system.

6. References

[1] Kuo B., Automatic Control Systems, 7th ed., New York: McGraw-Hill, pp.161-184, 2008.

[2] Draper C.S., Principles of Optimising Control Systems, 2nd ed., American Society of Mechanical Engineers, USA, pp.86, 1991.

[3] R.C. Dorf, Modern Control Systems, 3rd ed., New York, Addison-Wesley Publishing Company.

[4] Shinners J. S., Modern Control System Theory, 3rd ed., New York: McGraw-Hill, pp.190-203, 2004.

[5] PID Controller Design, Retrieved March 28, 2017, http://ctms.engin.umich.edu/CTMS/index.php?example=Introduction&section=ControlPID

[6] Euler Method, In Wikipedia. Retrieved January 8, 2017, from http://en.wikipedia.org/wiki/Euler_method

[7] Continuous-Discrete Conversion Methods. MathWorks R2014b Documentation. Retrieved January 18, 2017, http://www.mathworks.com/help/control/ug/continuous-discrete-conversion-methods.html#bs78nig-1

[8] Phillips C.L., Digital Control System, Prentice-Hall International Inc., UK London, pp.125-403, 2005.

[9] Yanev K.M., "Design and Analysis of a Robust Accurate Speed Control System by Applying a Digital Compensator", Journal of Automatic Control and System Engineering, USA, Volume 16, Issue 1, ISSN: 1687-4811, pp. 27-36, 2016.

[10] Cruise-Control; Retrieved January 18, 2017, from https://jagger.berkeley.edu/pack/me132/Section5.pdf

[11] Yanev K. M., "Application of the Method of D-Partitioning for Stability of Control Systems with Variable Parameters", BJT, Vol.16, Number 1, pp.51-58, 2007.

[12] Yanev K. M., "Analysis of Systems with Variable Parameters and Robust Controller Design", Proceedings of the Sixth IASTED International Conference on Modelling, Simulation and Optimization, MSO 2006, ISBN 088986-618-X, pp.75-83, 2006.

[13] Yanev K.M. Advanced D-Partitioning Stability Analysis in the 3-Dimensional Parameter Space, International Review of Automatic Control, ISSN: 1974-6059, Vol. 6, N. 3, pp. 236-240, 2013.

[14] Yanev K.M., Obok Opok, "Improved Technique of Multi-Stage Compensation", First African Control Conference AFRICON 2003, Cape Town, South Africa, p.S1-S6, 2003.

[15] Masupe S., Yanev K. M., "Design and D-Partitioning Analysis of Optimal Control System Compensation", Journal of International Review of Automatic Control, Vol. 4, N. 6, ISSN: 1974-6059, pp. 838-845, 2011.

[16] Tustin with Frequency Prewarping. MathWorks R2014b Documentation. Retrieved January 17, 2017,http://radio.feld.cvut.cz/matlab/toolbox/control/manipmod/ltiops20.html.

[17] Matched Z-transform method. In Wikipedia. Retrieved January 18, 2017, from http://en.wikipedia.org/wiki/Matched_Z-transform_method

[18] Yanev K. M., Anderson G. O., Masupe S., Strategy for Analysis and Design of Digital Robust Control Systems, ICGST-ACSE Journal, Volume 12, Issue 1, pp. 37-44, 2012.

[19] Abdala M. Alsharif M., DC Motor Drive System Cascade Control Strategy, Retrieved January 17, 2017, https://www.slideshare.net/RishikeshBagwe/dc-motor-drive-system-cascade-control-strategy

[20] Behera L., Kar I., Intelligent Systems and Control Principles and Applications, Oxford University Press, pp. 20-83, 2009.

[21] Yanev, K.M., Anderson G.O., Application of the D-partitioning for Analysis and Design of a Robust Photovoltaic Solar Tracker System, IJESCC, Volume 2, No. 1, pp. 43–54, 2011.

[22] Yanev, K.M., Anderson G.O., Masupe S., D-partitioning Analysis and Design of a Robust Photovoltaic Light Tracker System, BIE 12th Annual Conference, 6001, ISBN: 97899912-0-731-5, 2011.

[23] Yanev K.M., Advanced Interactive Tools for Analysis and Design of Nonlinear Robust Control Systems, International Review of Automatic Control, ISSN: 1974-6059, Vol. 6, N. 6, pp. 720-727, 2013.

[24] Yanev K. M, "Strategy for Design of Optimal Control System Compensation", International Journal of Energy Systems, Computers and Control, Vol. 1, No. 2, ISSN: 0976-6782, pp. 113–126, 2010.

[25] Bhanot S., Process Control Principles and Applications, Oxford University Press, pp. 170-187, 2010.

[26] Draper C.S., Principles of Optimizing Control Systems, 2nd ed., American Society of Mechanical Engineers, USA, pp.86, 1991.

[27] Dorf R.C., Modern Control Systems, 3rd ed., New York, Addison-Wesley Publishing Company,

[28] Yanev K.M., "Analysis of Systems with Variable Parameters and Robust Controller Design", Sixth IASTED International Conference on Modelling, Simulation and Optimization, p. 75-83, 2006.

[29] Click Charts Diagram & Flowchart Software Flexible Diagram Drawing and Creation, Retrieved March 28, 2017, from http://www.nchsoftware.com/chart/index.html?gclid=CJmBoOmkj9MCFTIW0wod9xsO_w

[30] Lucidchart.com - Lucidchart Official Site Retrieved March 28, 2017, from https://www.lucidchart.com/users/login?passwordOnly=1

[31] Flowchart Symbols Meaning Standard Flowchart Retrieved March 28, 2017, from http://creately.com/diagram-type/objects/flowchart

[32] Texas Instruments; TMS320F2837xS Delfino™ Microcontrollers; Retrieved March 28, 2017, from http://www.ti.com/lit/ds/symlink/tms320f28375s.pdf

Biographies

[1]Prof. Kamen Yanev has a M.Sc. in Control Systems Engineering. His Ph.D. is in the area of Systems with Variable Parameters and Robust Control Design. He started his academic career in 1974, following a number of academic promotions and being involved in considerable research, service and teaching at different Commonwealth Universities around the world. Prof. Yanev worked in a number of outstanding universities in Europe and in Africa, in countries like Nigeria, Zimbabwe and Botswana.

Currently he works as Associate Professor in Control and Instrumentation Engineering at the Department of Electrical Engineering at University of Botswana.

His major research is in the field of Automatic Control and Systems Engineering as well as in the subjects of Electronics and Instrumentation. He has 114 publications in international journals and conference proceedings in the area of Control Systems, Electronics, Instrumentation and Power Engineering.

Most of his latest publications and current research interests are in the field of Electronics, Analysis of Control Systems with Variable Parameters, Nonlinear and Digital Control Systems, Robust Control Design and Optimal Process Control Systems.

Prof. Yanev is interacting for many years with Saint-Cyr French Military Academy, supervising Military Academy students doing their M.Sc. dissertations.

He is a member of the Institution of Electrical and Electronic Engineering (IEEE), a Gold member of the Academic Community of International Congress for Global Science and Technology (ICGST), a member of the Instrumentation, Systems and Automation Society (ISA) and a member of the Botswana Institute of Engineers (BIE).

Prof. Yanev is also a member of the Editorial Board of the International Journal of Energy Systems, Computers and Control (IJESCC), at International Science Press, a member of the Editorial Board of the Journal of Multidisciplinary Engineering Science and Technology (JMEST), a reviewer for ACTA Press and a reviewer for Advances in Science, Technology and Engineering Systems Journal (ASTESJ), USA.